

CHEM MED CHEM

CHEMISTRY ENABLING DRUG DISCOVERY

Accepted Article

Title: Old Drug Scaffold, New Activity: Thalidomide Correlated Compounds Exerting Different Effects on Breast Cancer Cell Growth and Progression

Authors: Alessia Carocci, alessia catalano, Domenico Iacopetta, and Maria Stefania Sinicropi

This manuscript has been accepted after peer review and appears as an Accepted Article online prior to editing, proofing, and formal publication of the final Version of Record (VoR). This work is currently citable by using the Digital Object Identifier (DOI) given below. The VoR will be published online in Early View as soon as possible and may be different to this Accepted Article as a result of editing. Readers should obtain the VoR from the journal website shown below when it is published to ensure accuracy of information. The authors are responsible for the content of this Accepted Article.

To be cited as: *ChemMedChem* 10.1002/cmdc.201600629

Link to VoR: <http://dx.doi.org/10.1002/cmdc.201600629>

WILEY-VCH

www.chemmedchem.org

A Journal of



Old Drug Scaffold, New Activity: Thalidomide Correlated Compounds Exerting Different Effects on Breast Cancer Cell Growth and Progression

Dr. Domenico Iacopetta,^{a,§} Dr. Alessia Carocci,^{b,§} Prof. Maria Stefania Sinicropi,^{a,*} Dr. Alessia Catalano,^{b,*} Prof. Giovanni Lentini,^b Dr. Jessica Ceramella,^a Dr. Rosita Curcio,^a Prof. Maria Cristina Caroleo.^a

^a*Department of Pharmacy, Health and Nutritional Sciences, University of Calabria, 87036, Arcavacata di Rende, Italy*

^b*Department of Pharmacy-Drug Sciences, University of Bari "Aldo Moro", 70126, Bari, Italy.*

[§]These authors contributed equally to the paper.

*Corresponding authors:

Prof. Sinicropi Maria Stefania,
Department of Pharmacy, Health and Nutritional Sciences
University of Calabria
87036, Arcavacata di Rende, Italy
Phone: +39 0984 493200
E-mail: s.sinicropi@unical.it

Prof. Catalano Alessia
Department of Pharmacy-Drug Sciences
University of Bari "Aldo Moro"
70126, Bari, Italy
Phone: +39 080 5442745
E-mail: alessia.catalano@uniba.it

Abstract

Thalidomide was firstly used as morning sickness relief in pregnant women and then withdrawn from market because of its dramatic effects on fetal normal development. Over the last decades, it has been successfully used for the care of several pathologies, including cancer. Many analogues with improved activity were synthesized and tested. Herein, we report some effects on MCF-7 and MDA-MB-231 breast cancer cells growth and progression of a small series of thalidomide correlated compounds, very effective in inducing cancer cells death by triggering TNF α -mediated apoptosis. Moreover, the most active compounds are able, as well, to reduce drastically the migration of breast cancer cells, through the regulation of the two major proteins involved in epithelial-mesenchymal transition (EMT), vimentin and E-cadherin. They diminish the intracellular biosynthesis of vascular endothelial growth factor (VEGF), primarily involved in the promotion of angiogenesis that sustain tumor progression. The multiple features possessed by these compounds, acting on different key-points of tumorigenesis process, make them good candidates for preclinical studies.

Keywords: Thalidomide; Antitumor activity; TNF α ; Apoptosis; Angiogenesis.

Introduction

Thalidomide is a glutamic acid derivative synthesized in Germany in 1954 and marketed in 46 countries in the late 1950's and early 1960's as morning sickness relief in pregnant women.^[1] However, a massive increase of newborns with severe malformations (deafness, blindness, limb growth defects) was registered after thalidomide use, so that it was subsequently withdrawn in 1962.^[2] Over the last few decades the interest in this old drug has been renewed, because of its efficacy in several important diseases as, for instance, the erythema nodosum leprosum,^[3] multiple myeloma,^[4] breast cancer,^[5] refractory Crohn's disease^[6] and HIV-related diseases.^[7] It became clearer that thalidomide exerted multifaceted properties, leading many research groups to synthesize several derivatives and to study their effects, mostly in cancer research. Cancer growth and progression need fundamental changes, e.g. in energy metabolism pathways, in nutrient uptake and in several factors, leading to a phenotypic heterogeneity within subpopulations of cancer cells.^[8,9] These changes allow a higher ability to grow even in unsuited micro-environmental conditions (nutrient depletion, hypoxia).^[10] In 1994, D'Amato et al.^[11] reported that thalidomide was able to inhibit angiogenesis, induced in a rabbit cornea model, shedding light on the anti-angiogenic role responsible for teratogenicity. Remarkably, angiogenesis is essential for cancer growth, progression and metastasis and, amongst the pro-angiogenic factors, vascular endothelial growth factor (VEGF) plays a key role because of its up-regulation in tumors.^[12] Furthermore, many literature data showed that thalidomide inhibits tumor necrosis factor alpha (TNF α) production, which plays a dual role in cell proliferation, stimulating tumor cell growth or inducing cancer cell death.^[13] Starting from thalidomide, as a lead compound, several analogues have been developed, sharing and augmenting the antiproliferative, anti-angiogenic, and TNF α reducing properties of the parent compound.^[14-18] Another interesting thalidomide effect is the ability to inhibit the epithelial-mesenchymal transition (EMT), a dynamic process enabling polarized epithelial cells to assume a mesenchymal phenotype with enhanced migratory and invasive capabilities.^[19] EMT is associated with early stages of carcinogenesis, cancer invasion

and recurrence and is characterized by the reduction of epithelial cell junction proteins, including E-cadherin, α -catenin, claudins, occludin, combined with an increased expression of mesenchymal markers, such as *N*-cadherin, vimentin and fibronectin. In this context, it is of great interest to design and synthesize thalidomide analogues able to exert polyhedric effects on cancer cells proliferation.^[20,21] In this paper, we report the anti-tumor activity of some thalidomide analogues and correlated compounds (Figure 1), which are able to trigger cell death by TNF α -mediated apoptosis in two breast cancer cell lines, MCF-7 and MDA-MB-231, without affecting the proliferation of non-tumoral MCF-10a cells. Moreover, some of these compounds are able to reduce cancer cell migration, regulating the expression of two important proteins involved in epithelial-mesenchymal transition (EMT), namely E-cadherin and vimentin. We proved that these compounds possess a better activity and may represent a more effective drugs interfering with different breast tumor targets, thus offering a valid alternative in cancer treatment.

Chemistry.

Compounds **1**,^[22] **2**,^[23] **3**,**6**^[24] (Figure 1) were prepared as described elsewhere. Chiral compounds (**3**,**4**,**6**,**8**) were prepared in their racemic forms. Compound **4** was prepared as reported in Scheme 1. Compound **10** was readily prepared by the selectively Boc-protection of piperazine-2-carboxylic acid (**9**) at the 4-position, followed by Cbz-protection at the 1-position.^[25] Then, **10** was reacted with 2,6-dimethylaniline in the presence of IIDQ (2-isobutoxy-1-isobutoxycarbonyl-1,2-dihydroquinoline) to afford the corresponding carboxamide **11**.^[26] Selective Cbz-deprotection of **11** with triethylsilane and palladium chloride^[27] gave **12**, which was converted into the *N*-benzyl derivative **13** by reaction with benzyl bromide.^[28] Boc-deprotection of **13** and conversion of the resulted amine into the corresponding hydrochloride salt was performed with gaseous HCl as previously described.^[29] Compound **5** was synthesized as reported in Scheme 2 by reacting methyl imidazole-4-carboxylate (**14**) with 2,6-dimethylaniline according to a procedure reported in the literature.^[30] Compound **8** was synthesized as reported in Scheme 3. The amino alcohol **15**

was protected with phthalic anhydride^[31] to give the phthalimido alcohol **16** which was converted into the corresponding bromo derivative **8** by treatment with PBr₃.

Results and discussion

Antiproliferative activity

Thalidomide analogues were evaluated for their antiproliferative activities against two human breast cancer cell lines, namely estrogen receptor positive (ER+) MCF- and triple negative (ER-, PR-, and HER-2/Neu not amplified) MDA-MB-231 cells.^[32] Cells were subjected to 72 hours of continuous exposure to the tested compounds and, after that, their viability was measured by 3-(4,5-dimethylthiazol-2-yl)-2,5-diphenyltetrazolium (MTT) test.^[33,34] Thalidomide was used as reference molecule in these assays. The IC₅₀ values, *i.e.* the concentrations of the compounds producing the 50% of growth inhibition, are reported in Table 1. As shown, thalidomide exerted only a very poor antitumor activity in both the breast cell lines used, showing slight effects only at doses higher than 500 μM, whereas a very impressive activity was recorded with the synthesized compounds. Particularly, compounds **3** and **8** were the most active, with IC₅₀ values of 47 ± 1 μM and 40.3 ± 0.8 μM towards MCF-7 cells and 56.5 ± 1.3 μM and 37.2 ± 1.0 μM towards MDA-MB-213, respectively. The other compounds also showed interesting antiproliferative effects, even though to a lesser extent (see Table 1). Once established that our compounds possessed an improved antitumor activity with respect to thalidomide, we tested all the considered compounds on non-malignant breast epithelial cells, MCF-10a, in order to establish whether a cytotoxic effect could be exerted. We found that none the considered compounds produced toxic effects on the viability of normal breast epithelial cells up to 500 μM. The improved ability of our compounds to affect the proliferation of MCF-7 cells and, most importantly, of the highly aggressive and metastatic MDA-MB-231, without affecting non-tumoral breast epithelial cells MCF-10a, prompted us to investigate more deeply the properties of the most active compounds.

Cancer breast cells death by TNF α -mediated apoptosis

In previous reports, thalidomide was found to suppress TNF α mRNA expression.^[35] In this regard, literature data have clarified the complex interplay existing between TNF α and apoptosis, highlighting that TNF α can promote apoptotic cell death through the activation of several caspases and the mitochondrial damage, a pattern known as extrinsic apoptotic pathway. Hence, we investigated the ability of compounds **3** and **8** to modulate TNF α cell levels by immunofluorescence analysis. MCF-7 cells were exposed for 24 h to the two different compounds, at the concentrations equal to their own IC₅₀ values. Then cells were processed for immunofluorescence procedure using an antibody raised against TNF α vehicle-treated cells were used as a control. Immunofluorescence analysis of MCF-7 cells treated with the compounds **3** and **8** revealed a three- and two-fold increase of TNF α expression, respectively (Figure 2A and B). Furthermore, 2-(4-amidinophenyl)-6-indolecarbamide dihydrochloride (DAPI) staining of the same samples highlighted nuclei containing condensed DNA, frequently associated with apoptosis. It is known that the activation of the extrinsic apoptotic pathway implies an increased mitochondrial permeability, followed by the cytosolic release of cytochrome C, a small protein associated with the inner membrane of the intact mitochondria, that may act as apoptogenic factor.^[36] Therefore, we further investigated the subcellular localization of cytochrome C in MCF-7 cells treated with compounds **3** or **8**, using an antibody raised against cytochrome C (Figure 3A). It was remarkable that cytochrome C was released in the cytosol of the treated cells, as it can be evidenced by the increased and diffused fluorescence (Figure 3A and B), whereas in the vehicle-treated cells is still localized in the mitochondrial network. Moreover, TUNEL assay conducted on MCF-7 cells treated for 24 h with the compounds **3** or **8** revealed a green fluorescence in the cell nuclei, which indicates DNA fragmentation correlated with the apoptotic process (Figure 4). Taken together, our data highlight that compounds **3** and **8** are able to promote cancer breast cells death by increasing TNF α synthesis that, in turn, promotes cytochrome C release from mitochondria and, therefore, apoptosis.

Effects of compounds 1-8 on breast cancer cells migration

We tested the ability of compounds **1–8** to affect cell migration of MCF-7 and MDA-MB-231 cells by using a simple, low-cost and well-developed *in vitro* method, *i.e.* the wound-healing assay. Cells were plated and cultured to form a monolayer, then scratched to form a wound (see Experimental section) and treated with compounds **1–8** at the concentrations corresponding to their calculated IC_{50} (see Table 1) for 48 and 72 hours, respectively for MDA-MB-231 and MCF-7 cells. These different endpoint times were experimentally determined, considering that MDA-MB-231 cells possess a higher growth rate than the MCF-7 cells and tend to give greater metastases *in vivo*.^[37] In MCF-7 cells compounds **2**, **3**, **7** and **8** produced the higher effect, preventing the total wound closure, with percentages of about 52, 77, 72 and 69% (Figure 5A). In MDA-MB-231 cells, the above mentioned compounds **2**, **3**, **7** and **8** produced a significant lack of a total wound closure, respectively of about 11, 25, 27 and 25% but, differently from MCF-7 cells, compound **6** exhibited an impressive effect in prevent wound closure, of about 32% (Figure 5B). The other compounds had no significant effects in such experiments. In both breast cancer cell lines, compound **2** was the most effective in preventing the wound closure (Figure 3A and B) with respect to the other active compounds, but it possess a lesser efficacy in reducing cell viability, as demonstrated in our previous experiments (see Table 1). Overall, our data highlighted that compounds **3** and **8** showed a good activity in diminishing cancer cell migration (see Figure 5A and B, Figure 6), together with the lowest IC_{50} values (Table 1). Thus, we chose these two compounds for further investigations.

Compounds 3 and 8 hamper EMT decreasing breast cancer cells invasiveness

We firstly tried to better understand the role of compounds **3** and **8** in breast cancer cells invasion. Indeed, during EMT, malignant cells reorganize their cytoskeleton, expressing mesenchymal markers as vimentin, and lose inter-cellular adhesion molecules such as E-cadherin, which is considered as a diagnostic biomarker in breast cancer.^[38] In this regard, we tested the ability of

compounds **3** and **8** to modulate vimentin and E-cadherin levels in MCF-7 cells. Cells were exposed for 24 h to the compounds, used at the concentrations equal to their IC₅₀ values, processed and subjected to immunofluorescence analysis using antibodies against vimentin and E-cadherin. Vehicle-treated cells were used as a control. Immunofluorescence microscopy analysis showed that both compounds **3** and **8** strongly decreased vimentin levels (Figure 7A and B), at the same time, they significantly increased E-cadherin levels (Figure 8A and B), mostly at cytoplasmic membrane, where cell-cell interactions occur. These data indicate that compounds **3** and **8** may play a role in inhibiting EMT process, through the regulation of vimentin and E-cadherin expression, which are mainly involved in cancer invasion and metastases dissemination.

Compounds 3 and 8 are able to inhibit VEGF expression in cancer breast cells

Thalidomide is known to be a potent inhibitor of angiogenesis, an essential process in cancer cell proliferation, extracellular matrix invasion and metastasis. In 2006, Komorowski et al.^[39] reported that this drug could inhibit VEGF secretion in human endothelial cell line, decreasing neovascularization and VEGF can act as an autocrine or paracrine factor in the invasiveness of several cell types via receptor binding. On this basis, we tested by immunofluorescence studies whether compounds **3** and **8** could interfere with VEGF expression in MCF-7 cells. With this aim, MCF-7 cells were treated for 24 hours with compounds **3** or **8** (used at concentrations equal to their IC₅₀ values), and then subjected to immunofluorescence staining using an antibody raised against VEGF (Figure 9A). In such experiments, vehicle-treated cells were used as a control (CTRL). Interestingly, the fluorescent cytoplasmic signal correlated with the presence of VEGF was remarkably decreased in MCF-7 cells treated with both compounds **3** and **8**, with respect to the vehicle-treated cells (Figure 9A and B), indicating an interference with VEGF biosynthesis. This feature has been correlated, as well, with apoptosis induction in ER-positive and triple negative breast cancer cells, as already reported.^[40] Additionally, in MCF-7 cells treated with compound **8**, the decrease of VEGF-associated fluorescence is accompanied by an evident change

in subcellular localization (see Figure 9A, white arrows), which is no more evidently localized in the perinuclear area, as in the vehicle-treated cells, but diffused as well in the nuclei. This difference could indicate a decreased biosynthesis at the endoplasmic reticulum network and, at the same time, an interaction with nuclear receptors. VEGF nuclear accumulation may play several and still poorly understood roles, however Li et al.^[41] suggested a role in coagulation and fibrinolysis pathways, affecting vascular endothelial cellular physiology independently of its growth stimulation. The latter observation contrast with the results obtained by scratch and MTT assays, but further studies are needed in order to shed light on this feature. Summing up, our observations highlight the anti-angiogenic potential of these compounds, which represent one of the most desired feature of drugs used for the treatment of breast cancer.

Conclusions

The library of thalidomide correlated compounds reported in this paper consists of three newly synthesized compounds (**4**, **5** and **8**) and other already reported five thalidomide analogues (**1**, **2**, **3**, **6**, and **7**). The studied compounds have shown some interesting properties on breast cancer cells, particularly the estrogen-positive (ER+) MCF-7 and the triple negative MDA-MB-231 cells. Compared with their lead molecule, thalidomide, some of these compounds have shown a higher antitumor activity and, particularly, compounds **3** and **8** possess IC₅₀ values almost ten-fold lower than thalidomide. Besides, no significant cytotoxic effects have been noticed regarding MCF-10A normal breast cells viability. The antitumor effects have been ascribed to an intracellular increase of TNF α biosynthesis, which we believe is responsible for a protection mechanism (paracrine effect) against the abnormal proliferation of surrounding breast cancer cells. Indeed, this cytokine may trigger the apoptotic process through the mitochondrial pathway, given that a massive release of cytochrome c from the mitochondrial compartment to the cytosol has been detected by immunofluorescence assays. Cancer cell death by apoptosis has been definitely proved by TUNEL assay. Besides these effects on the breast cancer cells viability, compounds **3** and **8**, chosen to

further investigate other properties, are also able to decrease cancer cells migration and invasion, as demonstrated by wound healing assays. These features reside in the regulation of two major proteins involved in the EMT, *i.e.* vimentin and E-cadherin, which allow tumours cells to detach from the original site and disseminate through the blood vessels. The inhibition of vimentin biosynthesis and the increase of E-cadherin expression, induced by our compounds, represent a very interesting features, making cancer cell less prone to invasion and metastasis. Finally, compounds **3** and **8** may play a role in regulating VEGF expression in breast cancer cells, given that we have noticed a fall of VEGF intracellular levels and, as well, a different subcellular localization in cancer cells treated with compound **8**. In this regard, other studies are needed in order to better understand the precise mechanism responsible for the shown effects. However, we believe that these compounds possess a high potential, because of their multiple properties toward different aspects of breast cancer cell biology. Indeed, besides to their selective killing effect on cancer cells, the interference with the migration and invasion processes, which are the main cause of death for breast cancer patients, represent a peculiar and promising property. Lastly, the role played by our compounds in decreasing VEGF levels, mainly involved in the angiogenesis pathway responsible for promoting cancer survival, complete the sight of the multiple anticancer properties, exerted by our compounds. We are confident that our research will be seminal and encourage other studies on the design, development and biological evaluation of thalidomide correlated compounds.

Experimental section

Chemistry. All chemicals were purchased from Sigma-Aldrich or Lancaster in the highest quality commercially available. Solvents were reagent grade unless otherwise indicated. Yields refer to purified products and were not optimized. The structures of the compounds were confirmed by routine spectrometric analyses. Only spectra for compounds not previously described are given. Melting points were determined on a Gallenkamp melting point apparatus in open glass capillary

tubes and are uncorrected. ^1H NMR and ^{13}C NMR spectra were recorded on a Varian VX Mercury spectrometer operating at 300 and 75 MHz for ^1H and ^{13}C , respectively, or an Agilent 500 MHz operating at 500 and 125 MHz for ^1H and ^{13}C , respectively, using CDCl_3 and $\text{DMSO-}d_6$ as solvents. Chemical shifts are reported in parts per million (ppm) relative to solvent resonance: CDCl_3 , δ 7.26 (^1H NMR) and δ 77.0 (^{13}C NMR); $\text{DMSO-}d_6$, δ 2.48 (^1H NMR) and δ 39.9 (^{13}C NMR). J values are given in Hz. The following abbreviations are used: s-singlet, d-doublet, t-triplet. Gas chromatography (GC)/mass spectroscopy (MS) was performed on a Hewlett-Packard 6890–5973 MSD at low resolution. Elemental analyses were performed on a Eurovector Euro EA 3000 analyzer and the data for C, H, N were within ± 0.4 of theoretical values (Table S1). Chromatographic separations were performed on silica gel columns by flash chromatography (Kieselgel 60, 0.040–0.063 mm, Merck, Darmstadt, Germany) as previously described.^[42]

***N*-(2,6-Dimethylphenyl)piperazine-1-[(benzyloxy)carbonyl]-4-(tert-**

butoxycarbonyl)piperazine-2-carboxamide (11). IIDQ (0.27 mL, 0.92 mmol), 2,6-dimethylaniline (0.99 mL, 0.85 mmol) and Et_3N (0.16 mL, 1.15 mmol) were successively added to a stirring solution of compound **10** (0.28 g, 0.77 mmol) in CHCl_3 (26 mL). The reaction mixture was heated under reflux for 6 h. The solvent was removed under reduced pressure and the residue, taken up with EtOAc, was washed three times with 2 N HCl, twice with 2 N NaOH, and then dried over anhydrous Na_2SO_4 . Flash chromatography (eluent EtOAc/petroleum ether 4:6) of the residue gave 90 mg (25% yield) of **11** as a slightly yellowish oil: GC/MS (70 eV) m/z (%) 367 ($\text{M}^+ -100$, <1), 91 (100).

***tert*-Butyl 3-[(2,6-dimethylphenyl)carbamoyl]piperazine-1-carboxylate (12).** A suspension of compound **11** (80 mg, 0.17 mmol), triethylsilane (0.11 mL, 0.68 mmol), triethylamine (17 μL , 0.12 mmol), and PdCl_2 (9.03 mg, 0.051 mmol) in dichloromethane (1 mL) was heated at reflux for 3 h. The reaction mixture was quenched with saturated aqueous ammonium chloride solution and

extracted with ether several times. The combined organic phases were washed with water and then brine, dried, and concentrated in vacuo to give 45 mg (79%) of a slightly yellowish oil: GC/MS (70 eV) m/z (%) 333 (M^+ , 3), 129 (100).

***tert*-Butyl 4-benzyl-3-(2,6-dimethylphenylcarbamoyl)piperazine-1-carboxylate (13).** To a stirring solution of compound **12** (0.15 g, 0.45 mmol) in dioxane (8 mL), a solution of K_2CO_3 (0.18 g, 1.30 mmol) in H_2O (8 mL) was added. The reaction mixture was heated to 70 °C, and then, benzyl bromide (63 μ L, 0.53 mmol) was added dropwise. The heating was continued for 45 min. Then, the dioxane was removed under reduced pressure and the aqueous residue was taken up with EtOAc and extracted with 2 N HCl. The aqueous phase was made alkaline with 2 N NaOH and extracted twice with EtOAc. The combined organic layers were dried over anhydrous Na_2SO_4 and concentrated under vacuum to give 90 mg (47%) of a yellow oil: GC/MS (70 eV) m/z (%) 323 ($M^+ -100$, 2), 175 (100).

1-Benzyl-*N*-(2,6-dimethylphenyl)piperazine-2-carboxamide Hydrochloride (4·HCl).

Compound **4** as hydrochloride salt was obtained by saturating a solution of compound **13** in anhydrous Et_2O with gaseous HCl and stirring it at room temperature for 15 min. Removal of the solvent under reduced pressure gave a white solid (67%) which was recrystallized from EtOH/ Et_2O to afford white crystals: mp 235–237 °C (abs EtOH/ Et_2O); anal. calcd for $C_{12}H_{13}N_3O$: C 65.70, H 7.90, N 11.49, found: C 65.35, H 7.68, N 11.22.

***N*-(2,6-Dimethylphenyl)-1H-imidazole-4-carboxamide (5).** To a stirring suspension of 60% NaH (0.27 g, 6.67 mmol) in dry dioxane (10 mL) in N_2 atmosphere, 2,6-dimethylaniline (0.72 g, 5.95 mmol) was added and the mixture brought to reflux. Then, a solution of methyl imidazole-4-carboxylate (**14**, 0.30 g, 2.30 mmol) in dry DMF (13 mL) was added dropwise in an ice bath. After 5 h the mixture was poured into ice and extracted with EtOAc. The organic layer was then

evaporated *in vacuo*. Purification by column chromatography gave 0.26 g (53%) of **5** as a slightly yellowish solid: mp 212–214 °C; ¹H NMR (500 MHz, DMSO-*d*₆): δ 2.18 (s, 6H, CH₃), 3.77 (br s, 1H, NH), 7.05–7.15 (m, 3H, Ar), 8.57 (s, 1H, Ar), 9.18 (s, 1H, Ar), 10.5 (s, exch D₂O, 1H, NH); ¹³C NMR (125 MHz, DMSO-*d*₆): δ 18.6 (2C), 121.6 (1C), 127.6 (1C), 128.2 (1C), 128.3 (2C), 134.2 (2C), 135.9 (1C), 136.5 (1C), 156.1 (1C); GC/MS (70 eV) *m/z* (%) 215 (M⁺, 27), 121 (100); anal. calcd for C₁₂H₁₃N₃O: C 66.96, H 6.09, N 19.52, found: C 66.62, H 5.89, N 19.20.

2-(1-Hydroxy-3-methylbutan-2-yl)-1H-isoindole-1,3(2H)-dione (16).

A mixture of 2-amino-3-methylbutan-1-ol **15** (5 mmol), phthalic anhydride (5 mmol) and triethylamine (0.5 mmol) in 10 mL of toluene is heated under reflux in a flask fitted with a Dean–Stark tube for 3 h. During this period, the temperature of the oil bath is maintained at about 130°C and water separates. All volatile matter are then evaporated under vacuum and the solid residue is taken up with EtOAc and washed with 2N HCl, NaHCO₃, and H₂O. The organic phase is dried (Na₂SO₄) and concentrated under vacuum to give 0.56 g of **16** as a yellow oil (48%): GC/MS (70 eV) *m/z* (%) 233 (M⁺, 2), 202 (100).

2-(1-Bromo-3-methylbutan-2-yl)-1H-isoindole-1,3(2H)-dione (8).

PBr₃ (1.7 mmol) was carefully added to **16** (1.5 mmol) at 0 °C. The reaction mixture was stirred for 2 h at 0 °C and for 6 h at room temperature, then poured onto ice and extracted with AcOEt. The organic layer was washed with brine, dried over Na₂SO₄, and the solvent was evaporated *in vacuo* to give a pale-yellow oily residue. Purification by column chromatography (eluent EtOAc/hexane 2:8) gave 0.30 g (66%) of **8** as a white solid: ¹H NMR (500 MHz, CDCl₃): δ 0.91 (d, *J* = 6.4 Hz, 3H, CH₃), 1.08 (d, *J* = 6.4 Hz, 3H, CH₃), 2.36–2.46 (m, 1H, CHCH₃), 3.75–3.83 (m, 1H, CHN), 4.10–4.22 (m, 2H, CH₂), 7.68–7.78 (m, 2H, Ar), 7.82–7.90 (m, 2H, Ar); ¹³C NMR (125 MHz, CDCl₃): δ 20.3 (1C), 20.4 (1C), 30.4 (1C), 31.5 (1C), 59.6 (1C), 123.4 (2C),

131.5 (2C), 134.1 (2C), 168.4 (2C); GC/MS (70 eV) m/z (%) 296 (M^+ , 1), 252 (100); anal. calcd for $C_{13}H_{14}N_2OBr$: C 52.72, H 4.76, N 4.73, found: C 52.73, H 4.99, N 4.43.

Biology

Cell cultures. The three cell lines used in this work have been purchased from American Type Culture Collection (ATCC, Manassas, VA, USA). MCF-7 human breast cancer cells, estrogen receptor (ER) positives, were maintained in Dulbecco's Modified Eagle's Medium/Nutrient Mixture F-12 Ham (DMEM/F12), supplemented with 10% Foetal Bovine Serum (FBS) and 100 U/ml penicillin/streptomycin, as previously described.^[43] MCF-10a human mammary epithelial cells, were cultured in DMEM/F12 medium, supplemented with 5% Horse Serum (HS, (Eurobio, Les Ullis, Cedex, France), 100 U/ml penicillin/streptomycin, 0.5 mg/ml hydrocortisone, 20 ng/ml hEGF (human epidermal growth factor), 10 μ g/ml insulin and 0.1 mg/ml cholera enterotoxin (Sigma–Aldrich, Milano, Italy). MDA-MB-231 human breast cancer cells, known as triple negative cells (*i. e.* not overexpressing human epidermal growth factor receptor 2, or HER2, estrogen and progesterone receptors), were cultured in DMEM/F12, supplemented with 5% FBS, 1% L-glutamine and 100 U/ml penicillin/streptomycin. Cells were maintained at 37 °C in a humidified atmosphere of 95% air and 5% CO₂ and periodically screened for contamination.^[44] Thalidomide or its analogues were dissolved in dimethylsulfoxide (DMSO) (Sigma, St. Louis, Missouri, USA) and opportunely diluted in DMEM/F12 medium in order to obtain the working concentrations.

Cell viability. MDA-MB-231 and MCF-7 cells were grown in complete medium and, before being treated, they were starved in serum free medium for 24 h, to allow cell cycle synchronization. Then cells were grown in phenol red-free medium supplemented with 1% DCC (destran coated charcoal treated) FBS. Cells were treated with increasing concentrations (1, 5, 10, 25, 50, 100 and 500 μ M) of each compound for 72 h. Untreated cells were supplemented with the DMSO (final

concentration 0.1%) and used as a control.^[45] Cell viability was assessed using the 3-[4,5-dimethylthiazol-2-yl]-2,5-diphenyltetrazolium bromide reagent (MTT), according to the manufacturer's protocol (Sigma-Aldrich, Milan, Italy), as previously described.^[46] For each sample mean absorbance, measured at 570 nm, was expressed as a percentage of the control and plotted versus drug concentration to determine for each cell line the IC₅₀ values (i.e. drugs concentrations able to reduce cell viability of 50% with respect to the control), using GraphPad Prism 5 Software (GraphPad Inc., San Diego, CA). Mean values of three independent experiments carried out in triplicate and standard deviations (SD) are shown.

Wound-healing assay. MCF-7 and MDA-MB-231 cells were plated on 6-well plates and cultured in full medium to produce confluent monolayers. They were wounded in a line using a standard 200- μ l pipette sterile tip, then washed with PBS to remove cell debris before incubation with different concentrations of each compound at its IC₅₀, as indicated in table 1. Images at time zero (t = 0 h) were acquired to record the initial area of the wound, and the recovery of the wounded monolayer due to cells migration toward the scratched area was estimated at 48 and 72 h (t = Δ h). Images were captured using an inverted microscope equipped with digital camera (Leica DM 6000). The migration of cells toward the wounds was expressed as percentage of wound closure:

$$\% \text{ of wound closure} = [(A_{t=0 \text{ h}} - A_{t=\Delta \text{ h}}) / A_{t=0 \text{ h}}] \times 100\%,$$

Where, $A_{t=0 \text{ h}}$ is the area of wound measured immediately after scratching, and $A_{t=\Delta \text{ h}}$ is the area of wound measured 48 or 72 h after scratching. Vehicle-treated cells were used as a control. The collected images were analysed using Leica Application Suite X (LAS X) software. Each experiment was performed three times, and each treatment was conducted in three replicates. Representative images have been shown.

Tunel assay. Apoptosis was detected by the TUNEL assay, according to the guidelines of the manufacturer (CFTM488A TUNEL Assay Apoptosis Detection Kit, Biotium, Hayward, CA, USA), with some modifications.^[47] In brief, cells were grown on glass coverslips, after treatment, they were washed 3 times with PBS, then methanol-fixed at -20 °C for 15 min. Fixed cells were washed 3 times with 0.01% (V/V) Triton X-100 in PBS and incubated with 100 µL of TUNEL equilibration buffer for 5 min, then it was removed and 50 µL of TUNEL reaction mixture containing 1 µL of terminal deoxynucleotidyl transferase (TdT) were added to each sample and incubated in a dark and humidified chamber for 2 h at 37 °C. Samples were washed 3 times with ice cold phosphate-buffered saline (PBS) containing 0.1% Triton X-100 and 5 mg/mL bovine serum albumin (BSA). DAPI (0.2 µg/mL) counterstain was performed for 10 min at 37 °C in dark and humidified conditions. Cells were then washed 3 times with cold PBS, adding one drop of mounting solution, then they were observed and imaged under a fluorescence microscope (Leica DM 6000) (20X magnification) with excitation/emission wavelength maxima of 490 nm/515 nm (CFTM488A) or 350 nm/460 nm (DAPI). Images are representative of three independent experiments.

Immunofluorescence. For immunocytochemistry, cells were grown on coverslips in full media, then serum-starved for 24 h for the indicated time with examined compounds. Then they were PBS-washed and fixed with cold methanol (15 min/-20 °C) and washed 3 times (10 min/room temperature) with cold PBS containing 0.01 % TritonX-100. After incubation (30 min/room temperature) with blocking solution (PBS, 2% BSA), they were incubated with primary antibodies diluted in blocking solution (4°C/overnight). The primary antibody raised against E-Cadherin (4065) and the antibody raised against vimentin (3932) were purchased from Cell Signaling (Cell Signaling technology, MI, Italy) and both used at 1:100 dilution, anti-TNFα (52B83) and anti-VEGF (A-20), acquired from Santa Cruz Biotechnology Inc. (Santa Cruz, CA, USA), were used at 1:50 and 1:100 dilutions, respectively, furthermore the purified mouse anti-cytochrome C

(556433) was purchased from BD Biosciences and used at 1:100 dilution. Coverslips were then washed 3 times with PBS, then fixed cells were incubated with the secondary antibodies Alexa Fluor® 568 conjugate goat-anti-mouse or *Alexa Fluor® 488 conjugate* goat-anti-rabbit (both used at 1:500 dilution and acquired from Thermo Fisher Scientific, MA USA). Nuclei were stained using DAPI (Sigma) for 10 min at a concentration of 0.2 µg/mL then washed 3 times with PBS. Fluorescence was detected using a fluorescence microscope (Leica DM 6000). LASX software was used to acquire and process all images.^[48]

Statistical analysis

Data were analysed for statistical significance ($p < 0.001$) using One-way ANOVA followed by Dunnett's test performed by Graph Pad Prism 5. Standard deviations (SD) are shown.

Acknowledgment. This work was supported by MIUR to M.S. Sinicropi. We would like to thank Dr. Noemi Muià for her technical support.

Abbreviations used

ANOVA, Analysis of Variance; DAPI, 2-(4-amidinophenyl)-6-indolecarbamide dihydrochloride; DMEM/F12, Dulbecco's Modified Eagle Medium F12; EMT, epithelial-mesenchymal transition; FBS, Fetal Bovine Serum; IIDQ, 2-isobutoxy-1-isobutoxycarbonyl-1,2-dihydroquinoline; MCF-7, Michigan Cancer Foundation-7; MCF-10A, Michigan Cancer Foundation-10A; MDA-MB-231, M.D. Anderson Metastatic Breast-231; MTT, Methylthiazol Tetrazolium Assay; TNF α , tumor necrosis factor alpha; TUNEL, Terminal deoxynucleotidyl transferase dUTP nick end labeling; VEGF, vascular endothelial growth factor.

References

- [1] N. Vargesson, *Birth Defects Res. C Embryo Today* **2015**, *105*, 140–156.
- [2] J. H. Kim, A. R. Scialli, *Toxicol. Sci.* **2011**, *122*, 1–6.

- [3] J. J. Wu, D. B. Huang, K. R. Pang, S. Hsu, S. K. Tying, *Br J Dermatol* **2005**, *153*, 254–273.
- [4] X. Wang, Y. Li, X. Yan, *Biomed. Res. Int.* **2016**, 6848902.
- [5] B. Y. A. El-Aarag, T. Kasai, M. A. H. Zahran, N. I. Zakhary, T. Shigehiro, S. C. Sekhar, H. S. Agwa, A. Mizutani, H. Murakami, H. Kakuta, M. Seno, *Internat. Immunopharmacol.* **2014**, *21*, 283–292.
- [6] M. Simon, B. Pariente, J. Lambert, J. Cosnes, Y. Bouhnik, P. Marteau, M. Allez, J. F. Colombel, J. M. Gornet, *Clin. Gastroenterol. Hepatol.* **2016**, *14*, 966–972.e2.
- [7] P. Charles, C. Richaud, S. Beley, L. Bodard, M. Simon, *J. Clin. Virol.* **2016**, *78*, 12–13.
- [8] A. Caruso, D. Iacopetta, F. Puoci, A. R. Cappello, C. Saturnino, M. S. Sinicropi, *Mini Rev. Med. Chem.* **2016**, *16*, 630–643.
- [9] D. Iacopetta, Y. Rechoum, S. A. Fuqua, *Drug Discov. Today Dis. Mech.* **2012**, *9*, e19–e27.
- [10] R. G. Jones, C. B. Thompson, *Genes Dev.* **2009**, *23*, 537–548.
- [11] R. J. D'Amato, M. S. Loughnan, E. Flynn, J. Folkman, *Proc. Natl Acad. Sci. USA* **1994**, *91*, 4082–4085.
- [12] P. Carmeliet, *Oncology* **2005**, *69*, 4–10.
- [13] X. Wang, Y. Lin, *Acta Pharmacol. Sin.* **2008**, *29*, 1275–1288.
- [14] C. Chaulet, C. Croix, D. Alagille, S. Normand, A. Delwail, L. Favot, J. C. Lecron, M. C. Viaud-Massuard, *Bioorg. Med. Chem. Lett.* **2011**, *21*, 1019–1022.
- [15] G. W. Muller, L. G. Corral, M. G. Shire, H. Wang, A. Moreira, G. Kaplan, D. I. Stirling, *J. Med. Chem.* **1996**, *39*, 3238–3240.
- [16] G. W. Muller, M. G. Shire, L. Min Wong, L. G. Corral, R. T. Patterson, Y. Chen, D. I. Stirling, *Bioorg. Med. Chem.* **1998**, *8*, 2669–2674.
- [17] M. Gütschow, T. Hecker, A. Thiele, S. Hauschildt, K. Eger, *Bioorg. Med. Chem.* **2001**, *9*, 1059–1065.
- [18] E. R. Lepper, S. S. W. Ng, M. Gütschow, M. Weiss, S. Hauschildt, T. K. Hecker, F. A. Luzzio, K. Eger, W. D. Figg, *J. Med. Chem.* **2004**, *9*, 2219–2227.
- [19] H. Arai, A. Furusu, T. Nishino, Y. Obata, Y. Nakazawa, M. Nakazawa, M. Hirose, K. Abe, T. Koji, S. Kohno, *Acta Histochem. Cytochem.* **2011**, *44*, 51–60.
- [20] M. A. Huber, N. Kraut, H. Beug, *Curr. Opin. Cell Biol.* **2005**, *17*, 548–558.
- [21] A. J. Trimboli, K. Fukino, A. de Bruin, G. Wei, L. Shen, S. M. Tanner, N. Creasap, T. J. Rosol, M. L. Robinson, C. Eng, M. C. Ostrowski, G. Leone, *Cancer Res.* **2008**, *68*, 937–945.
- [22] A. Catalano, R. Luciani, A. Carocci, D. Cortesi, C. Pozzi, C. Borsari, S. Ferrari, S. Mangani, *Eur. J. Med. Chem.* **2016**, *123*, 649–664.
- [23] C. Lamanna, A. Catalano, A. Carocci, A. Di Mola, C. Franchini, V. Tortorella, P. M. Vanderheyden, M. S. Sinicropi, K. A. Watson, S. Sciabola, *ChemMedChem* **2007**, *2*, 1298–1310.
- [24] A. Carocci, G. Lentini, A. Catalano, M. M. Cavalluzzi, C. Bruno, M. Muraglia, N. A. Colabufo, N. Galeotti, F. Corbo, R. Matucci, C. Ghelardini, C. Franchini, *ChemMedChem* **2010**, *5*, 696–704.
- [25] C. F. Bigge, S. J. Hays, P. M. Novak, J. T. Drummond, G. Johnson, T. P. Bobovski, *Tetrahed. Lett.* **1989**, *30*, 5193–5196.
- [26] A. Catalano, A. Carocci, F. Corbo, C. Franchini, M. Muraglia, A. Scilimati, M. De Bellis, A. De Luca, D. Conte Camerino, M. S. Sinicropi, V. Tortorella, *Eur. J. Med. Chem.* **2008**, *43*, 2535–2540.
- [27] A. Catalano, A. Carocci, G. Lentini, A. Di Mola, C. Bruno, C. Franchini, *J. Heterocycl. Chem.* **2011**, *48*, 261–266.
- [28] M. Muraglia, M. De Bellis, A. Catalano, A. Carocci, C. Franchini, A. Carrieri, C. Fortugno, C. Bertucci, J. F. Desaphy, A. De Luca, D. C. Camerino, F. Corbo, *J. Med. Chem.* **2014**, *57*, 2589–2600.

- [29] A. Catalano, A. Carocci, M. M. Cavalluzzi, A. Di Mola, G. Lentini, A. Lovece, A. Dipalma, T. Costanza, J. F. Desaphy, D. Conte Camerino, C. Franchini, *Arch. Pharm. Chem. Life. Sci.* **2010**, *343*, 325–332.
- [30] S. Miyano, K. Sumoto, F. Satoh, K. Shima, M. Hayashimatsu, M. Morita, K. Aisaka, T. Noguchi, *J. Med. Chem.* **1985**, *28*, 714–717.
- [31] A. Catalano, R. Budriesi, C. Bruno, A. Di Mola, I. Defrenza, M. M. Cavalluzzi, M. Micucci, A. Carocci, C. Franchini, G. Lentini, *Eur. J. Med. Chem.* **2013**, *65*, 511–516.
- [32] G. Palma, G. Frasci, A. Chirico, E. Esposito, C. Siani, C. Saturnino, C. Arra, G. Ciliberto, A. Giordano, M. D'Aiuto, *Oncotarget* **2015**, *6*, 26560-26574.
- [33] E. Sirignano, A. Pisano, A. Caruso, C. Saturnino, M. S. Sinicropi, R. Lappano, A. Botta, D. Iacopetta, M. Maggiolini, P. Longo, *Anticancer Agents Med. Chem.* **2015**, *15*, 468–474.
- [34] O. I. Parisi, C. Morelli, F. Puoci, C. Saturnino, A. Caruso, D. Sisci, G. E. Trombino, N. Picci, M. S. Sinicropi, *J. Mat. Chem. B* **2014**, *2*, 6619–6625.
- [35] A. L. Moreira, E. P. Sampaio, A. Zmuidzinas, P. Frindt, K. A. Smith, G. Kaplan, *J. Exp. Med.* **1993**, *177*, 1675–1680.
- [36] J. C. Yang, G. A. Cortopassi, *Free Radic. Biol. Med.* **1998**, *24*, 624–631.
- [37] P. Rizza, M. Pellegrino, A. Caruso, D. Iacopetta, M. S. Sinicropi, S. Rault, J. C. Lancelot, H. El-Kashef, A. Lesnard, C. Rochais, P. Dallemagne, C. Saturnino, F. Giordano, S. Catalano, S. Ando, *Eur. J. Med. Chem.* **2016**, *107*, 275–287.
- [38] R. Singhai, V. W. Patil, S. R. Jaiswal, S. D. Patil, M. B. Tayade, A. V. Patil, *N. Am. J. Med. Sci.* **2011**, *3*, 227–233.
- [39] J. Komorowski, H. Jerczynska, A. Siejka, P. Baranska, H. Lawnicka, Z. Pawlowska, H. Stepien, *Life Sci.* **2006**, *78*, 2558–2563.
- [40] T. H. Lee, S. Seng, M. Sekine, C. Hinton, Y. Fu, H. K. Avraham, S. Avraham, *PLoS Med.* **2007**, *4*, e186.
- [41] W. L. Li, G. A. Keller, *J. Cell Sci.* **2000**, *113*, 1525–1534.
- [42] A. Carocci, A. Catalano, C. Bruno, G. Lentini, C. Franchini, M. De Bellis, A. De Luca, D. Conte Camerino, *Chirality* **2010**, *22*, 299–307.
- [43] A. Chimento, M. Sala, I. M. Gomez-Monterrey, S. Musella, A. Bertamino, A. Caruso, M. S. Sinicropi, R. Sirianni, F. Puoci, O. I. Parisi, C. Campana, E. Martire, E. Novellino, C. Saturnino, P. Campiglia, V. Pezzi, *Bioorg. Med. Chem. Lett.* **2013**, *23*, 6401–6405.
- [44] E. Sirignano, C. Saturnino, A. Botta, M. S. Sinicropi, A. Caruso, A. Pisano, R. Lappano, M. Maggiolini, P. Longo, *Bioorg. Med. Chem. Lett.* **2013**, *23*, 3458–3462.
- [45] M. S. Sinicropi, A. Caruso, F. Conforti, M. Marrelli, H. El Kashef, J. C. Lancelot, S. Rault, G. A. Statti, F. Menichini, *J. Enzyme Inhib. Med. Chem.* **2009**, *24*, 1148–1153.
- [46] A. Carocci, A. Catalano, C. Bruno, A. Lovece, M. G. Roselli, M. M. Cavalluzzi, F. De Santis, A. De Palma, M. R. Rusciano, M. Illario, C. Franchini, G. Lentini, *Bioorg. Med. Chem.* **2013**, *21*, 847–851.
- [47] D. Iacopetta, C. Rosano, F. Puoci, O. I. Parisi, C. Saturnino, A. Caruso, P. Longo, J. Ceramella, A. Malzert-Freon, P. Dallemagne, S. Rault, M. S. Sinicropi, *Eur. J. Pharm. Sci.* **2016**, *96*, 263–272.
- [48] D. Iacopetta, R. Lappano, A. R. Cappello, M. Madeo, E. M. De Francesco, A. Santoro, R. Curcio, L. Capobianco, V. Pezzi, M. Maggiolini, V. Dolce, *Breast Cancer Res. Treat.* **2010**, *122*, 755–764.

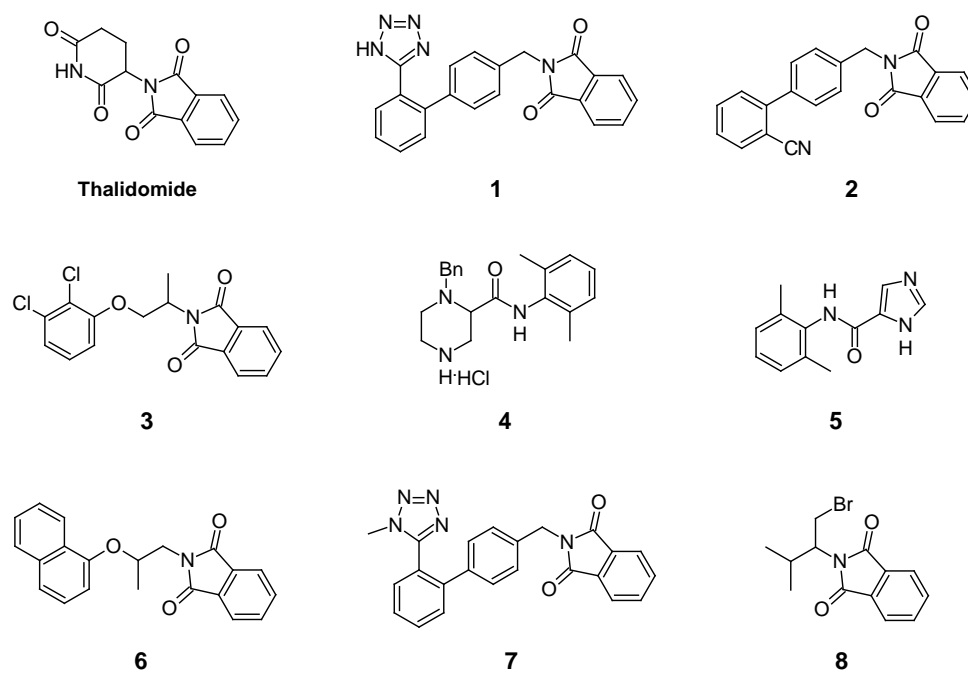
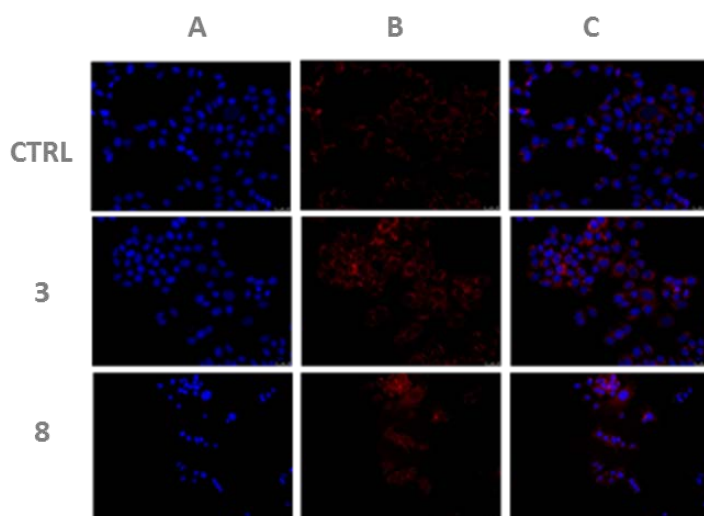
Figure 1. Structures of thalidomide and correlated compounds

Figure 2. A) Immunofluorescence analysis of TNF α levels in MCF-7 cells. Cells were treated for 24 h with compounds **3** and **8** or vehicle (CTRL), then processed as described in Experimental section. Images were acquired at 20X magnification. Panel A: DAPI; Panel B: Alexa Fluor 568; Panel C: Overlay. Images are representative of three separate experiments. B) Fluorescence quantification is shown. *** $p < 0.001$.

A



B

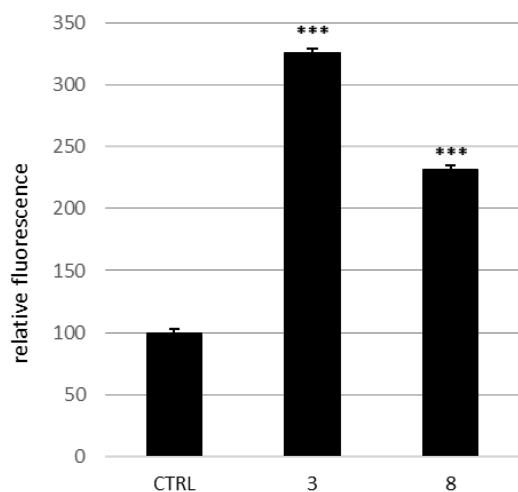
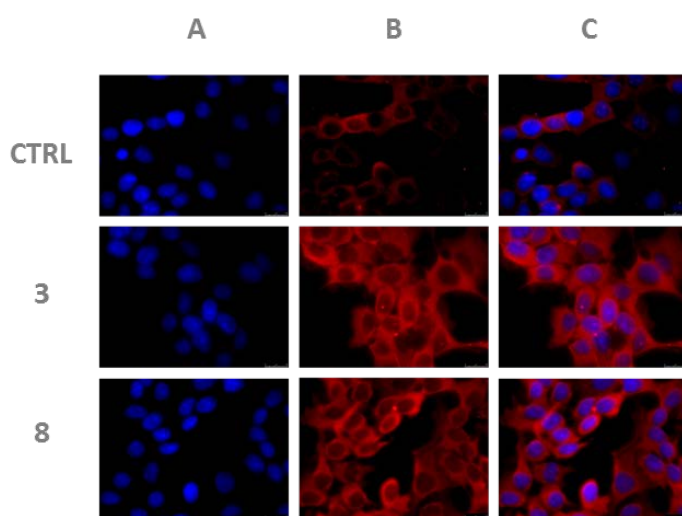


Figure 3. A) Immunofluorescence analysis of cytochrome c. MCF-7 cells were treated for 24 h with compounds **3** or **8**, or with vehicle (CTRL). Images were acquired at 63X magnification. Panel A: DAPI; Panel B: Alexa Fluor 568; Panel C: Overlay. Images are representative of three separate experiments. B) Fluorescence quantification is shown. *** $p < 0.001$.

A



B

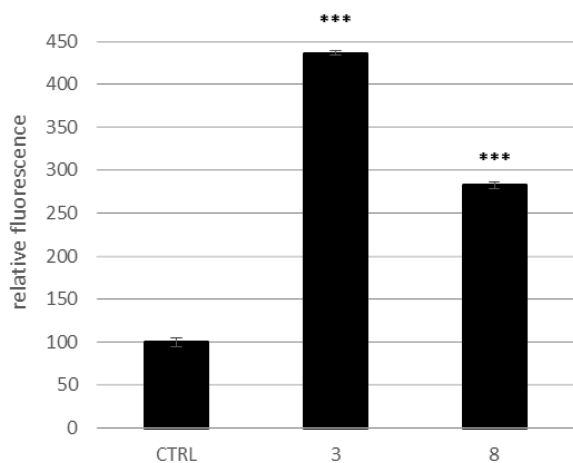


Figure 4. Apoptosis detection by TUNEL assay on MCF-7 breast cancer cells. Cells were treated for 24 h with compounds **3** and **8**, then cold methanol fixed and subjected to TUNEL procedure. Then, cells have been washed, dyed with DAPI and observed and imaged under an inverted fluorescence microscope (20X magnification). Panels A: CFTM488A; Panels B: DAPI; Panels C: Overlay. Representative fields are shown.

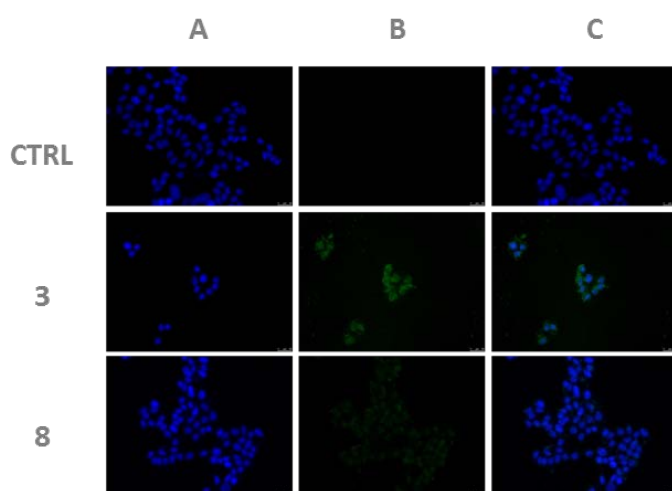


Figure 5. Wound-healing assay conducted on MCF-7 (A) and MDA-MB-231 (B) cells treated with compounds **1-8**. Wound closure was monitored recording the area of the cell-free wound at time 0h and 72h for MCF-7 and at time 0h and 48h for MDA-MB-231, by the use of an inverted microscope. The wound healing effect was estimated as the percentage of wound closure calculated as reported in material and method section. Vehicle-treated (CTRL) cells were used as a control. *** $p < 0.001$.

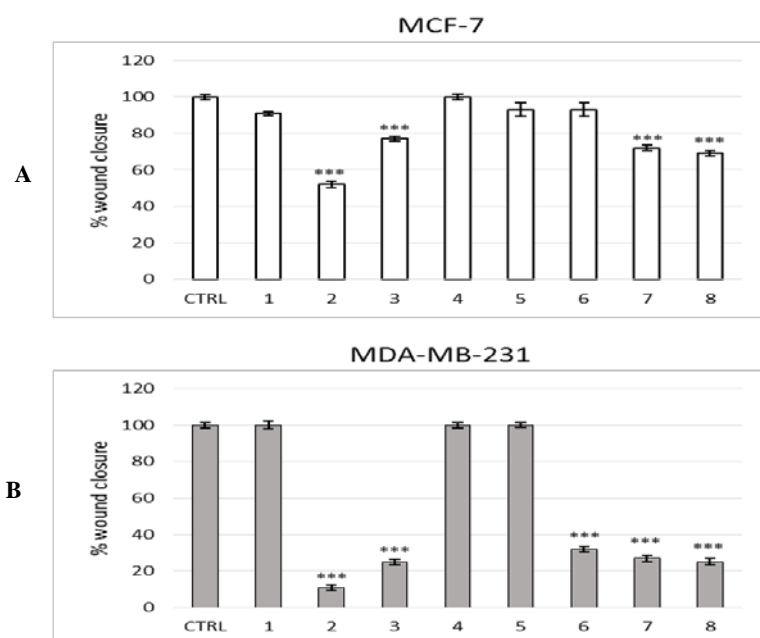


Figure 6. Wound-healing assay conducted on MCF-7 (A) and MDA-MB-231 (B) cells plated on six-well plates and treated with compounds **3** or **8** and vehicle (CTRL). Wound closure was monitored at times 0h and 72h for MCF-7 and at times 0h and 48h for MDA-MB-231, by the use of an inverted microscope (5X magnification). The dotted red lines define the areas lacking cells.

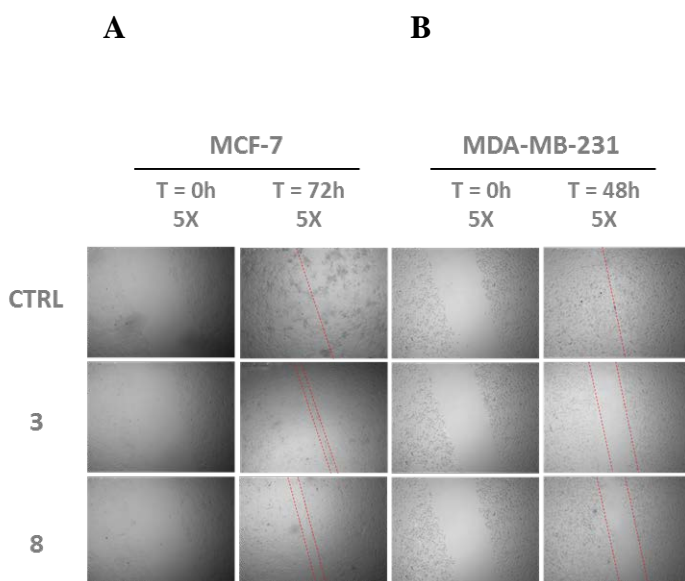
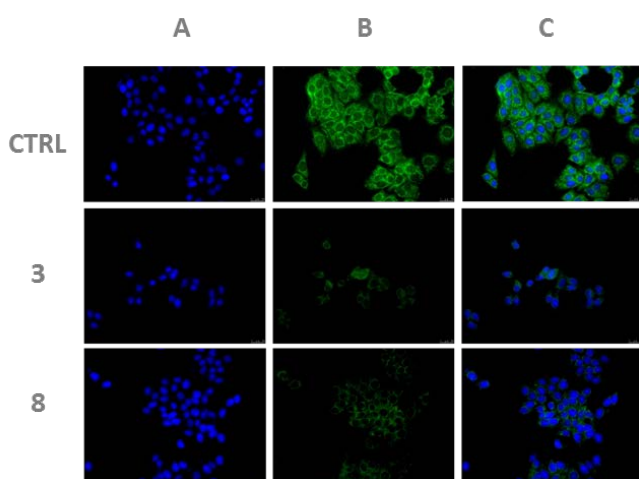
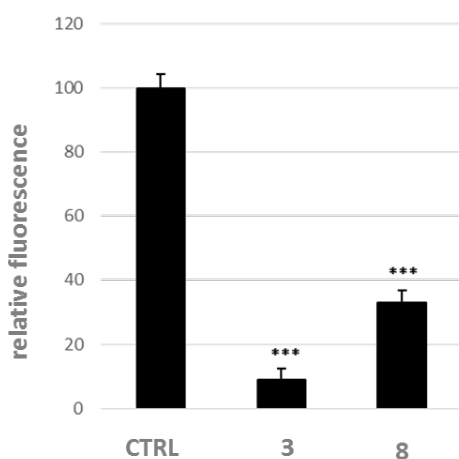


Figure 7. Immunofluorescence analysis of vimentin. A) MCF-7 cells were treated for 24h with compounds **3**, **8** or vehicle (CTRL). Images were acquired at 20X magnification. Panel A: DAPI; Panel B: Alexa Fluor® 488; Panel C: Overlay. Images are representative of three separate experiments. B) Fluorescence quantification, *** $p < 0.001$.

A



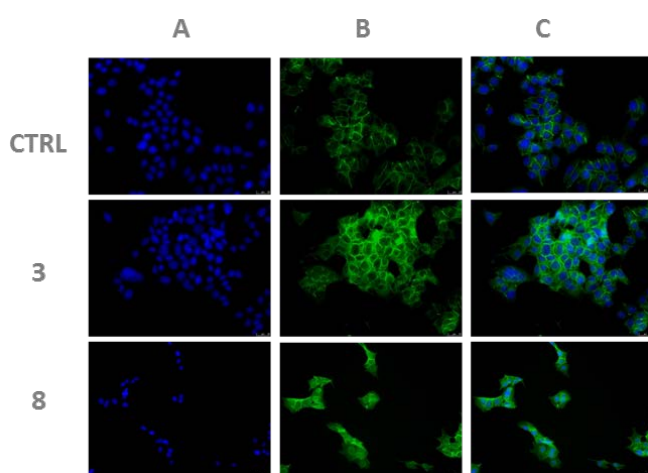
B



Accepted Manuscript

Figure 8. Immunofluorescence analysis of E-cadherin. A) MCF-7 cells were treated for 24h with compounds **3**, **8** or vehicle (CTRL). Images were acquired at 20X magnification. Panel A: DAPI; Panel B: Alexa Fluor® 488; Panel C: Overlay. Images are representative of three separate experiments. B) Fluorescence quantification, *** p<0.001.

A



B

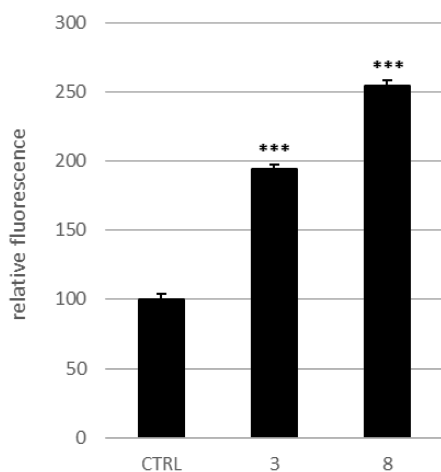
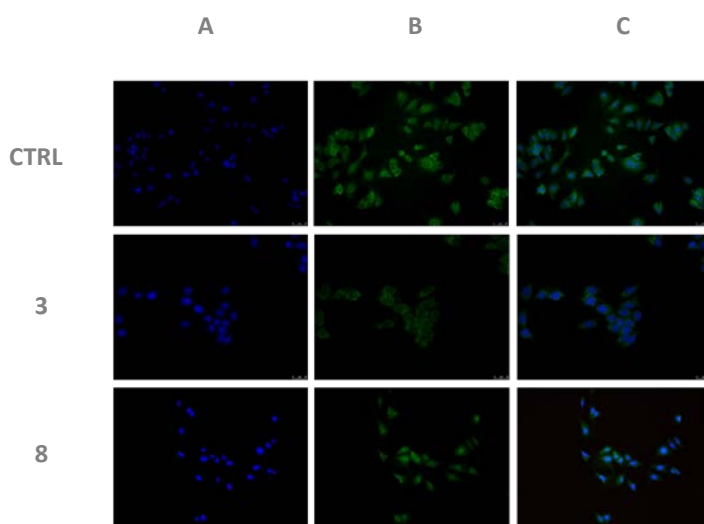
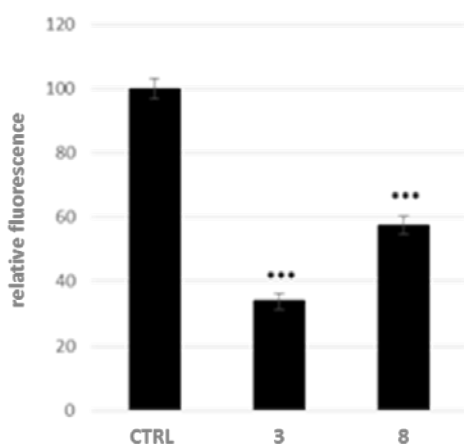


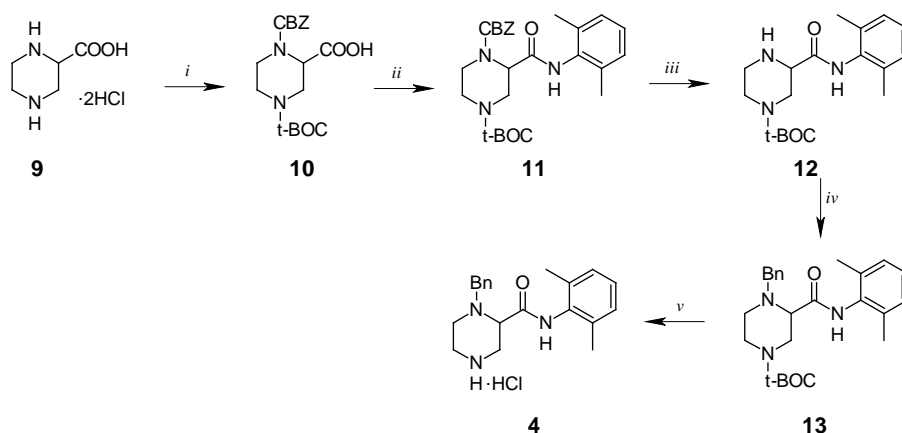
Figure 9. Immunofluorescence analysis of VEGF. A) MCF-7 cells were treated for 24 h with compounds **3**, **8** or vehicle (CTRL). White arrows indicate the different subcellular localization of VEGF in MCF-7 cells treated with compound **8**, with respect to the vehicle treated cells (CTRL). Images were acquired at 20X magnification. Panel A: DAPI; Panel B: Alexa Fluor® 488; Panel C: Overlay. Images are representative of three separate experiments. B) Fluorescence quantification, *** $p < 0.001$.

A

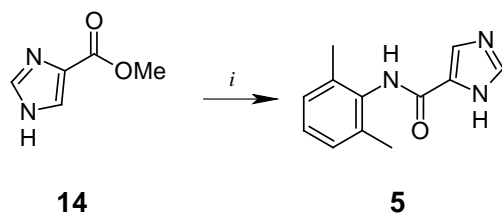


B

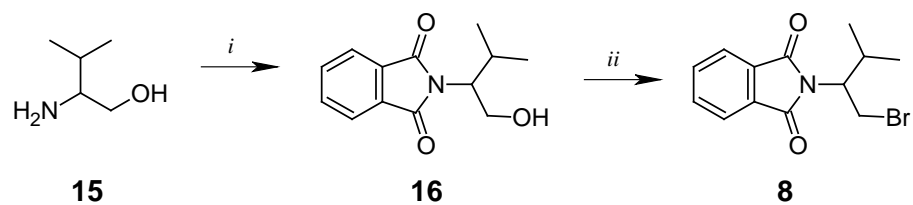


Scheme 1. Synthesis of compound **4**

Reagents and conditions: (i) Boc-ON, benzylchloroformate, dioxane/water, rt; (ii) 2,6-dimethylaniline, IIDQ, Et₃N, CHCl₃, reflux; (iii) Et₃SiH, PdCl₂, Et₃N, CH₂Cl₂, reflux; (iv) BnBr, K₂CO₃, dioxane/water, 70 °C; (v) g. HCl, anhyd Et₂O, rt.

Scheme 2. Synthesis of compound **5**

Reagents and conditions: (i) 2,6-dimethylaniline, NaH, dry dioxane/dry DMF, reflux.

Scheme 3. Synthesis of compound **8**

Reagents and conditions: (i) phthalic anhydride, triethylamine, toluene, reflux; (ii) PBr₃, 0 °C then rt.

Table 1. IC₅₀ values of thalidomide and compounds **1–8**

	IC ₅₀ (μM) ^a		
	MCF-7	MDA-MB-231	MCF-10A
Thalidomide	360 ± 2	413 ± 2	> 500
1	293.8 ± 1.0	> 500	> 500
2	99.6 ± 1.2	165.5 ± 1.8	> 500
3	47 ± 1	56.5 ± 1.3	> 500
4	204.8 ± 0.7	119.3 ± 1.8	> 500
5	> 500	> 500	> 500
6	302.6 ± 2.1	151.9 ± 1.6	> 500
7	57.3 ± 2.2	80.9 ± 2.2	> 500
8	40.3 ± 0.8	37.2 ± 1.0	> 500

^aValues are the mean of three independent experiments performed in triplicate and standard deviations (SD) are shown.

Accepted Manuscript

Figure captions

Figure 1. Structures of thalidomide and correlated compounds

Figure 2. A) Immunofluorescence analysis of TNF α levels in MCF-7 cells. Cells were treated for 24 h with compounds **3** and **8** or vehicle (CTRL), then processed as described in Experimental section. Images were acquired at 20X magnification. Panel A: DAPI; Panel B: Alexa Fluor 568; Panel C: Overlay. Images are representative of three separate experiments. B) Fluorescence quantification is shown. *** p<0.001.

Figure 3. A) Immunofluorescence analysis of cytochrome c. MCF-7 cells were treated for 24 h with compounds **3** or **8**, or with vehicle (CTRL). Images were acquired at 63X magnification. Panel A: DAPI; Panel B: Alexa Fluor 568; Panel C: Overlay. Images are representative of three separate experiments. B) Fluorescence quantification is shown. *** p<0.001.

Figure 4. Apoptosis detection by TUNEL assay on MCF-7 breast cancer cells. Cells were treated for 24 h with compounds **3** and **8**, then cold methanol fixed and subjected to TUNEL procedure. Then, cells have been washed, dyed with DAPI and observed and imaged under an inverted fluorescence microscope (20X magnification). Panels A: CFTM488A; Panels B: DAPI; Panels C: Overlay. Representative fields are shown.

Figure 5. Wound-healing assay conducted on MCF-7 (A) and MDA-MB-231 (B) cells treated with compounds **1-8**. Wound closure was monitored recording the area of the cell-free wound at time 0h and 72h for MCF-7 and at time 0h and 48h for MDA-MB-231, by the use of an inverted microscope. The wound healing effect was estimated as the percentage of wound closure calculated as reported in material and method section. Vehicle-treated (CTRL) cells were used as a control. *** p<0.001.

Figure 6. Wound-healing assay conducted on MCF-7 (A) and MDA-MB-231 (B) cells plated on six-well plates and treated with compounds **3** or **8** and vehicle (CTRL). Wound closure was

monitored at times 0h and 72h for MCF-7 and at times 0h and 48h for MDA-MB-231, by the use of an inverted microscope (5X magnification). The dotted red lines define the areas lacking cells.

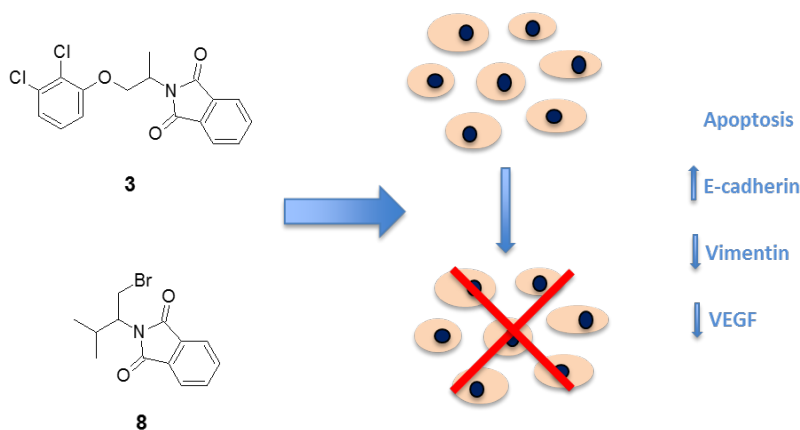
Figure 7. Immunofluorescence analysis of vimentin. A) MCF-7 cells were treated for 24h with compounds **3**, **8** or vehicle (CTRL). Images were acquired at 20X magnification. Panel A: DAPI; Panel B: Alexa Fluor® 488; Panel C: Overlay. Images are representative of three separate experiments. B) Fluorescence quantification, *** $p < 0.001$.

Figure 8. Immunofluorescence analysis of E-cadherin. A) MCF-7 cells were treated for 24h with compounds **3**, **8** or vehicle (CTRL). Images were acquired at 20X magnification. Panel A: DAPI; Panel B: Alexa Fluor® 488; Panel C: Overlay. Images are representative of three separate experiments. B) Fluorescence quantification, *** $p < 0.001$.

Figure 9. Immunofluorescence analysis of VEGF. A) MCF-7 cells were treated for 24 h with compounds **3**, **8** or vehicle (CTRL). White arrows indicate the different subcellular localization of VEGF in MCF-7 cells treated with compound **8**, with respect to the vehicle treated cells (CTRL). Images were acquired at 20X magnification. Panel A: DAPI; Panel B: Alexa Fluor® 488; Panel C: Overlay. Images are representative of three separate experiments. B) Fluorescence quantification, *** $p < 0.001$.

Table of Contents

Old Drug Scaffold, New Activity: Thalidomide Correlated Compounds Exerting Different Effects on Breast Cancer Cell Growth and Progression



Compounds **3** and **8** act on different key-points of tumorigenesis process by drastically reducing the migration of breast cancer cells, through the regulation of vimentin and E-cadherin and by diminishing the intracellular biosynthesis of VEGF.